Ice I_h revisited: No proton tunneling observed in a quasielastic neutron scattering experiment

Alexander I. Kolesnikov,[1,*] Georg Ehlers,[2] Eugene Mamontov,[1] and Andrey Podlesnyak[1]
[1]*Neutron Scattering Division, Oak Ridge National Laboratory, Oak Ridge, Tennessee 37831, USA*
[2]*Neutron Technologies Division, Oak Ridge National Laboratory, Oak Ridge, Tennessee 37831, USA*

(Received 25 April 2018; revised manuscript received 5 July 2018; published 7 August 2018)

A large broadening (∼0.4 meV) of quasielastic neutron scattering (QENS) signal in H_2O ice I_h at $T = 5$ K was observed by Bove *et al.* [Phys. Rev. Lett. **103**, 165901 (2009)] and explained by a model of concerted proton tunneling. This result was rather unexpected, as prior studies never showed significant mobility in water at low temperatures and ambient pressure. There were a few attempts of theoretical understanding of the effect. Recent path-integral simulations as well as quantum lattice-gauge theory supported the possibility of the collective tunneling of protons in ice I_h, however other studies stated that concerted tunneling in ice I_h should have very low frequency. Here, we report on QENS measurements of H_2O ice I_h at 1.8 and 5 K by using neutron scattering spectrometers with the energy resolution similar to and four times better than the energy resolution in the original experiment of Bove and co-workers. We did not observe any QENS broadening, and the measured spectra for the ice I_h and the reference vanadium sample were almost identical. Therefore, we conclude that there is no proton tunneling in ice I_h at temperatures down to 1.8 K measurable on an energy scale of 3.5 μeV and above. The literature data on low-temperature heat capacity of ice I_h support this conclusion.

DOI: 10.1103/PhysRevB.98.064301

Significance of quantum effects in water has been well recognized (see, e.g., [1–10]). Quantum tunneling in water is very important to understand its many anomalous properties, but the estimated tunneling rates in ordinary ice I_h, or energy splitting of the ground state, are rather small. In the case of water proton translational tunneling in ice I_h from one molecule to another along the hydrogen bond, the tunneling distance is ∼0.84 Å and the potential barrier is of the order of O-H covalent bond (∼400 kJ/mol or 4 eV). The tunneling splitting of the ground state (of energy E_G) in the double-well potential $U(x)$ can be expressed as [11]

$$E_{tun} \approx \hbar\omega \exp\left(-\frac{1}{\hbar}\int \sqrt{2m[U(x)-E_G]}\,dx\right), \quad (1)$$

where $\hbar\omega$ is the energy of the intramolecular O-H stretching mode (about 410 meV), and the corresponding proton tunneling rate in ice I_h at low temperature is expected to be negligibly small, about a few MHz, similar to what was recently observed in a hexamer water cluster [4]. The proton tunneling is predicted to be much faster in high-pressure ice phases, when under pressure the O-O distance between water molecules significantly decreases (<2.45 Å, as in ice VII at $P > 50$ GPa), and the covalent O-H bond determining the barrier height decreases (due to increase of the hydrogen bond), and a water proton can be described as a proton in a shallow double-well potential with a small distance between the minima. Path-integral simulations successfully describe a transition from the proton-ordered structure ice VIII to a proton-disordered phase ice VII by applying a high pressure, owing to translational proton tunneling [9,12,13].

A recent observation of a broad (full width at half maximum, FWHM ≈ 0.4 meV) quasielastic neutron scattering (QENS) signal in H_2O ice I_h at $T = 5$ K [14], by using IRIS spectrometer at ISIS (RAL) with moderate energy resolution 15 μeV, has attracted much attention. The QENS signal was explained by a model of concerted proton tunneling in proton-ordered six water molecule rings. The simultaneous concerted proton tunneling does not create new ion defects in ice and does not violate the Bernal-Fowler ice rules [15]. The intensity of the observed QENS signal was rather large, about 4% of the intensity of the elastic line, and this value is close to the statistical appearance (1/32) of the proton ordered six-member ring in the proton disordered ice I_h. The QENS measurement with H_2O ice I_h doped with 20% D_2O did not show the QENS broadening [14] in agreement with expected statistical disturbance of the proton-ordered six-member rings by deuterium atoms. There were a few attempts of theoretical understanding of the effect.

Recent *ab initio* path-integral simulations [16–18], as well as quantum lattice-gauge theory [19], supported the possibility of the collective tunneling of six protons in proton-ordered six-member rings in ice I_h at low temperature. However, other studies [9,20] noted that due to long O-O distance concerted tunneling in ice I_h should have very low frequency, as we mentioned above.

Due to the fundamental importance of the phenomenon observed in [14], in this study we performed QENS measurements of H_2O ice I_h by using CNCS (at $T = 1.8$ K) [21,22] and BASIS (at $T = 5$ K) [23] spectrometers at the Spallation Neutron Source (SNS) at Oak Ridge National Laboratory, with respective energy resolution similar to and four times better than the energy resolution in the original experiment [14]. The CNCS is a direct geometry time-of-flight spectrometer, and we used incident neutron energy $E_i = 1$ meV and the

*Corresponding author: kolesnikovai@ornl.gov

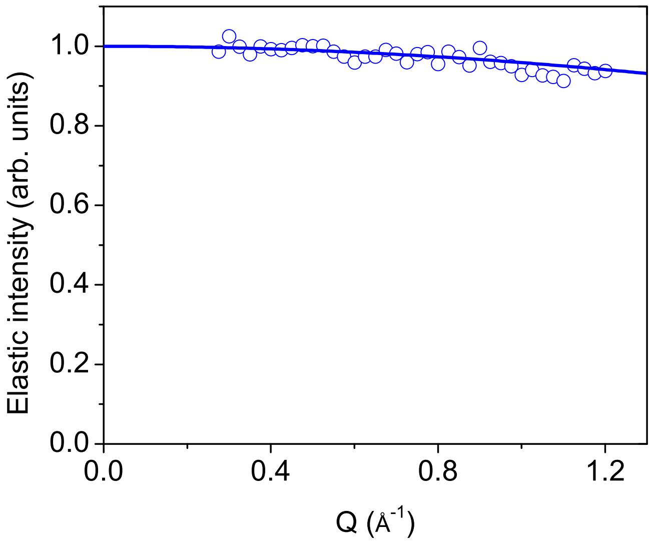

FIG. 1. Wave-vector dependence of the elastic contribution (EISF) of ice I_h from CNCS measurements with a wavelength of 9.045 Å. The detector array at CNCS extends to scattering angles up to 133°, which means that a Q range up to 1.2 Å^{-1} is covered.

neutron choppers setting, which provides energy resolution of 18 μeV. The BASIS is an inverse geometry backscattering spectrometer, and we used different neutron analyzing crystals, Si(111) and Si(311), which provide respectively energy resolution of 3.5 and 10 μeV, and an energy window $\pm$200 and $\pm$700 μeV. To suppress multiple neutron scattering the deionized water was placed in a cylindrical hollow (annular) aluminum container (1.2 cm diameter and 5 cm height) with sample thickness of 100 μm. The spectra from a vanadium foil of similar shape were also measured as a resolution function of the spectrometers at the same spectrometers' settings and temperatures. The sample and vanadium data were corrected for background measured from the empty container. The collected QENS data were reduced using MANTID [24] and DAVE [25] software packages.

The elastic intensity (elastic incoherent structure factor, EISF) for ice I_h shows the Debye-Waller dependence (see Fig. 1, for the data obtained at CNCS), thus demonstrating that the spectra indeed represent the incoherent scattering signal from the sample. At CNCS, an incident neutron energy $E_i = 1$ meV was used, corresponding to a neutron wavelength $\lambda = 9.045$ Å, which is larger than twice the value of the largest d spacing of ice I_h, aluminum, or vanadium, and therefore no Bragg peaks can be visible.

There is no visible QENS broadening of the ice I_h spectra in all three different measurements. In order to improve statistics, we have integrated the spectra over neutron momentum transfer Q. Figure 2 shows the QENS spectra of H_2O ice I_h and vanadium (as spectrometer resolution) measured at BASIS [panels (a) and (b)] and CNCS [panel (c)] spectrometers. To get the quantitative information on possible QENS component, the experimental spectra were fitted to a standard model consisted of a δ function describing the elastic scattering, a single Lorentzian function accounting for the QENS signal, and a linear sloped background, all convoluted with the instrumental resolution function:

$$I(E) = \left(A_0 \delta(E) + \frac{A_1}{\pi} \frac{\Gamma}{\Gamma^2 + E^2} \right) \otimes R(E) + C_1 E + C_2, \tag{2}$$

where E is neutron energy transfer, A_0 and A_1 are the integrated intensity of the δ function and the Lorentzian component, respectively, Γ is the half width at half maximum of the Lorentzian, $R(E)$ is a resolution function (represented by the vanadium spectrum), and C_1 and C_2 are the slope and the intercept of the linear background. The values of the free parameters are determined by a least-squares fit to the experimental data. The fit quality is good, but the fits refuse

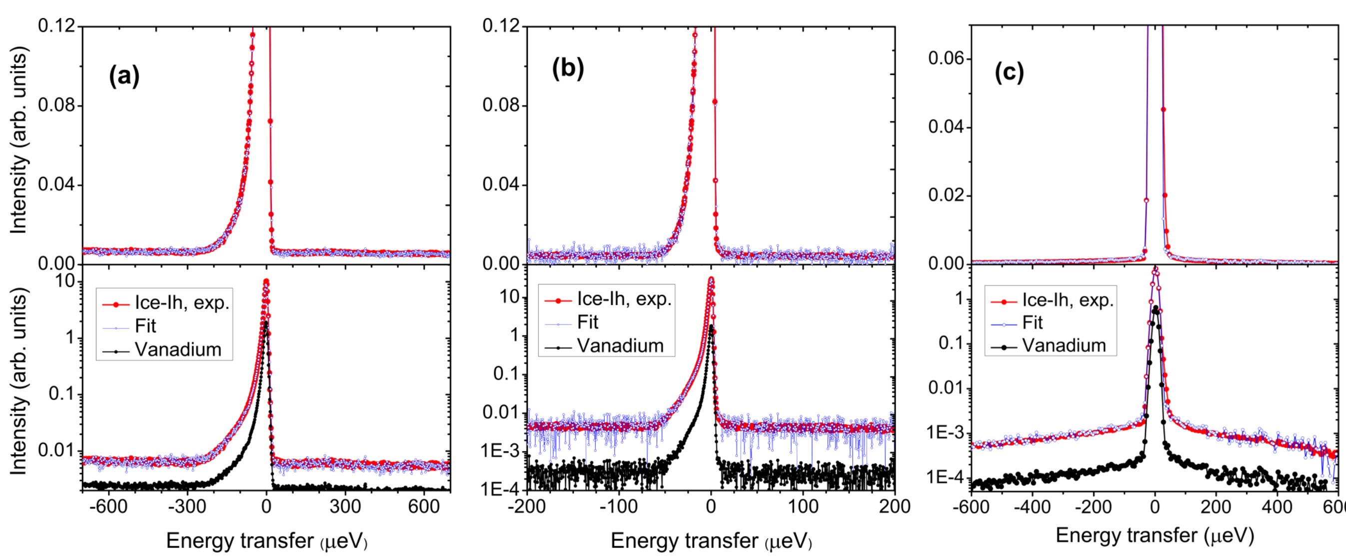

FIG. 2. QENS spectra of ice I_h (red curves) and vanadium (as a resolution of spectrometer, black curves in the bottom panels), measured at BASIS at $T = 5$ K with analyzer crystals: (a) Si(311) with energy resolution 10 μeV, (b) Si(111) with energy resolution 3.5 μeV, and (c) at CNCS at $T = 1.8$ K with incident neutron energy $E_i = 1$ meV and with energy resolution 18 μeV. The top and bottom panels are for linear and logarithmic scales, respectively; the blue curves show the fit spectra.

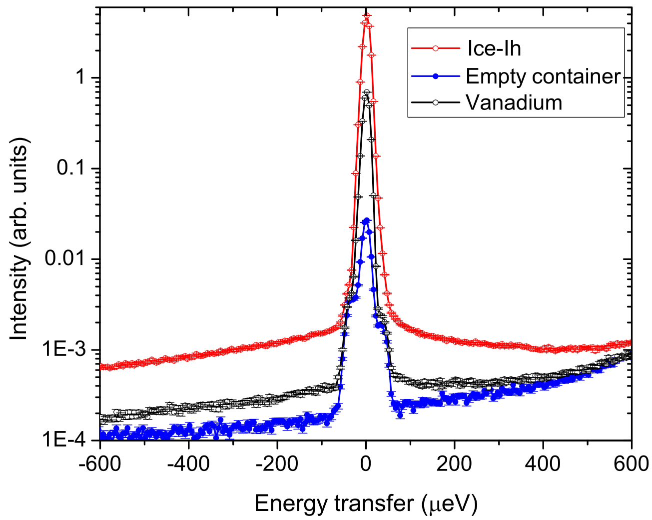

FIG. 3. Raw neutron scattering spectra of empty aluminum annular container in He cryostat, and ice I_h and vanadium (both in the same container), measured at CNCS at $T = 1.8$ K with incident neutron energy $E_i = 1$ meV. The signal of raw ice I_h spectrum is more than 100 times larger than for empty container. Two shoulders at the elastic line in the empty container spectrum and also on raw vanadium spectrum are visible, which are due to neutron scattering on front and back walls of the inner part of the cryostat, but subtraction of the empty container spectrum completely removes them (see Fig. 2).

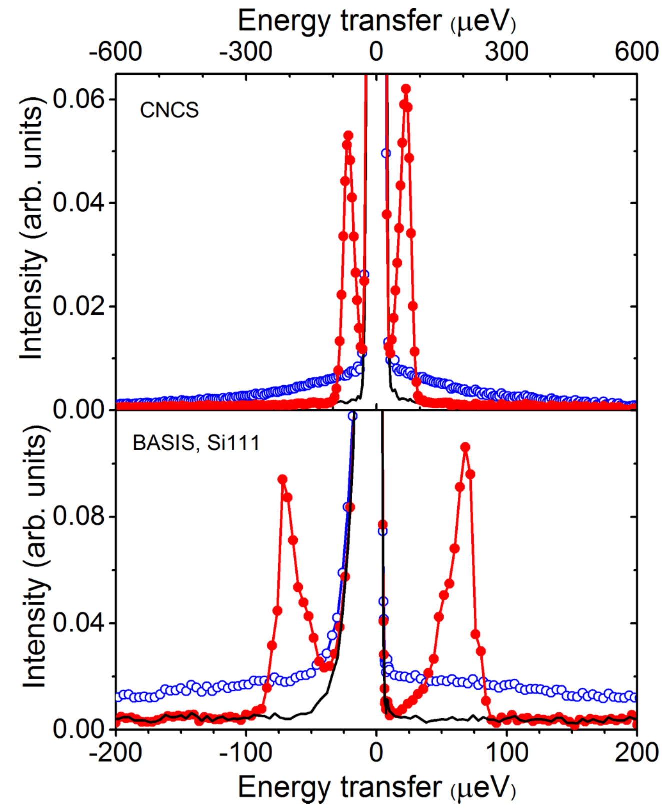

FIG. 4. Inelastic neutron scattering spectra (top and bottom panels for CNCS and BASIS, respectively) calculated assuming the elastic line (delta function, weight of 96%) plus either tunneling peaks, based on the model of hydrogen tunneling in ice I_h [19] (red spectra) or Lorentzian QENS line with FWHM = 0.4 meV [14] (blue spectra), both having weight of 4%, all are convoluted with the experimental spectrometers resolution functions. The black curve shows the elastic line only.

to accommodate the Lorentzian contribution at all (either its area becomes zero, or the error on its width greatly exceeds the width value). In the case of the CNCS data set (energy window ± 600 μeV), the fit results in a positively sloping background. In the case of BASIS, the fit of the data collected with Si(111) analyzers [energy window ± 200 μeV, and the analyzing (final) energy $E_f = 2.08$ meV] requires only a flat background, and the fit of the data taken with Si(311) analyzers (energy window ± 700 μeV, and $E_f = 7.64$ meV) requires a slightly negatively sloping background. The presence of the positively and negatively sloping background around the elastic line in $I(E)$ spectra collected with direct and inverse geometry time-of-flight spectrometers, respectively, can be explained by the transformation Jacobian from the time-of-flight to energy-transfer data, $I(E) = I(t)\frac{dt}{dE}$, which can be expressed as being proportional to $[1 + \frac{3}{2}\frac{E}{E_i} + \frac{15}{8}(\frac{E}{E_i})^2 + \cdots]$ or $[1 - \frac{3}{2}\frac{E}{E_f} + \frac{15}{8}(\frac{E}{E_f})^2 - \cdots]$, respectively for the former and latter cases, assuming $\frac{E}{E_i} \ll 1$ and $\frac{E}{E_f} \ll 1$. Therefore, if the collected time-of-flight $I(t)$ data contain a time-independent background (due to cosmic x rays and/or electronic noise in the detectors) then it will be presented as a sloping background in the $I(E)$ data around the elastic line.

The raw neutron scattering spectra of ice I_h, vanadium, and an empty aluminum container in a helium cryostat clearly show this kind of background (see Fig. 3). Besides the sample-independent background (e.g., due to sample environment scattering, and time independent background), which ideally can be subtracted from the sample signal, there is also sample-dependent background in the range of QENS signal, which increases with the scattering from the sample itself (e.g., from the contribution by inelastic processes, like lattice acoustic modes, which extends too far away from the elastic line to be resolved explicitly). Such background can never be subtracted and necessitates the use of a background term in the fits. This background is, in general, sloped, because the underlying effects that cause it are not symmetric in energy transfer. Nevertheless, a quasielastic process, which is associated with a symmetric line shape (except for the small detailed balance effect), is always distinguishable in fits from a sloped background, as long as it is not too narrow for the resolution line and not too broad for the accessible range of energy transfers. It is for this reason that we used spectrometers with variable energy resolution and energy transfer range; none of the measurements could find any evidence of a quasielastic processes, even in the fits.

If 4% of protons in H_2O ice I_h could perform concerting tunneling at low temperatures with the tunneling states shown in Fig. 9 of Ref. [19] (which were proposed in order to describe the QENS spectra observed in ice I_h [14]), then this tunneling should be also observable in our spectra. Figure 4 shows the inelastic neutron scattering spectra calculated assuming either the model of hydrogen tunneling in ice I_h, based on the calculations [19] with the tunneling mode of 0.062 meV or Lorentzian QENS line with FWHM = 0.4 meV [14], both

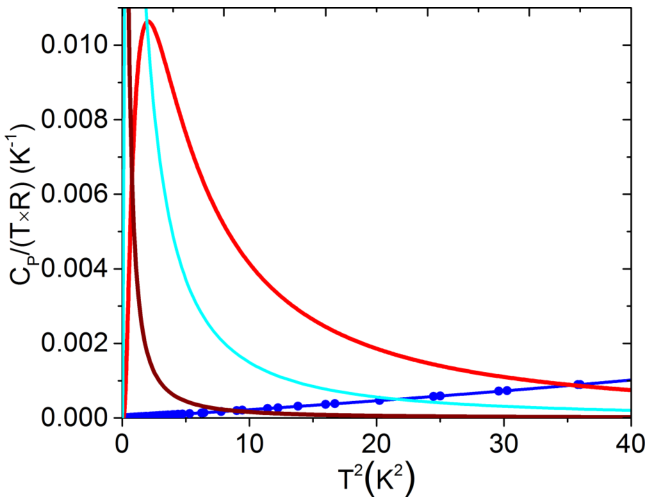

FIG. 5. Heat capacity of ice I_h at low temperatures (blue points and curve) [26] and calculated contribution to $C_P(T)$ due to presence of 4% of two-level states (Schottky anomaly) with splitting energy $\Delta E = 0.4$, 0.2, and 0.062 meV (red, cyan, and wine curves, respectively); $R = 8.3145$ J mol^{-1} K^{-1} is the universal gas constant.

having weight 4%, plus elastic line (δ function) weight of 96%, all are convoluted with the experimental spectrometer resolution functions. It is clear that the tunneling peaks or quasielastic signal with the used energies and width, and especially the spectral weight as reported in [14], should be readily identifiable in the QENS spectra of ice I_h measured at BASIS and CNCS, if they were present.

A possible presence of the tunneling modes in ice I_h should be as well reflected in the heat-capacity data $C_P(T)$ at low temperatures. The lowest temperature $C_P(T)$ data for H_2O ice I_h available in the literature (down to 0.5 K [26]) show no anomaly in the temperature range 0.5–10 K, where the $C_P(T)$ follows the dependence $\sim T^3$, as it should be for dielectric material with Debye behavior for vibrational density of states at low energies. The tunneling splitting of the water ground state, described as a two-level energy state (TLE) with energy splitting ΔE, would contribute to heat capacity at low temperature as

$$C_{\rm TLE}(T) = N_{\rm TLE} k_{\rm B} \frac{\left(\frac{\Delta E}{k_{\rm B}T}\right)^2 \exp\left(\frac{\Delta E}{k_{\rm B}T}\right)}{\left[1+\exp\left(\frac{\Delta E}{k_{\rm B}T}\right)\right]^2}, \quad (3)$$

where $N_{\rm TLE} = 0.04$ is a number of TLE states and $k_{\rm B}$ is a Boltzmann constant. Figure 5 shows the experimental $C_P(T)$ for ice I_h [26] and the calculated contribution of TLE states if the tunneling of water protons existed. We used $\Delta E = 0.4$ and 0.2 meV (corresponding to full and half value of FWHM of QENS component in [14]), and also $\Delta E = 0.062$ meV, the tunneling peaks calculated in [19]. The experimental data certainly disagree with the calculated $C_{\rm TLE}(T)$, even for the lowest $\Delta E = 0.062$ meV, indicating nonexistence of tunneling in ice I_h with the parameters used in the calculation.

In summary, we have measured QENS spectra of H_2O ice I_h at temperatures 1.8 and 5 K and did not observe any QENS broadening. Therefore, we conclude that there is no proton tunneling in ice I_h at temperatures down to 1.8 K measurable on the energy scale of 3.5 μeV ($\sim$1 GHz) and above.

Research at Oak Ridge National Laboratory's Spallation Neutron Source was supported by the Scientific User Facilities Division, Office of Basic Energy Sciences, US Department of Energy. This paper has been authored by UT-Battelle, LLC, under Contract No. DE-AC05-00OR22725 with the US Department of Energy. The United States Government retains and the publisher, by accepting the article for publication, acknowledges that the United States Government retains a nonexclusive, paid-up, irrevocable, worldwide license to publish or reproduce the published form of this paper, or allow others to do so, for United States Government purposes.

The Department of Energy will provide public access to these results of federally sponsored research in accordance with the DOE Public Access Plan [27].

[1] J. Guo, X.-Z. Li, J. Peng, E.-G. Wang, and Y. Jiang, Atomic-scale investigation of nuclear quantum effects of surface water: Experiments and theory, Prog. Surf. Sci. **92**, 203 (2017).

[2] M. Ceriotti, W. Fang, P. G. Kusalik, R. H. McKenzie, A. Michaelides, M. A. Morales, and T. E. Markland, Nuclear quantum effects in water and aqueous systems: Experiment, theory, and current challenges, Chem. Rev. **116**, 7529 (2016).

[3] A. I. Kolesnikov, G. F. Reiter, N. Choudhury, T. R. Prisk, E. Mamontov, A. Podlesnyak, G. Ehlers, A. G. Seel, D. J. Wesolowski, and L. M. Anovitz, Quantum Tunneling of Water in Beryl: A New State of the Water Molecule, Phys. Rev. Lett. **116**, 167802 (2016).

[4] J. O. Richardson, C. Pérez, S. Lobsiger, A. A. Reid, B. Temelso, G. C. Shields, Z. Kisiel, D. J. Wales, B. H. Pate, and S. C. Althorpe, Concerted hydrogen-bond breaking by quantum tunneling in the water hexamer prism, Science **351**, 1310 (2016).

[5] A. L. Agapov, A. I. Kolesnikov, V. N. Novikov, R. Richert, and A. P. Sokolov, Quantum effects in the dynamics of deeply supercooled water, Phys. Rev. E **91**, 022312 (2015).

[6] C. Gainaru, A. L. Agapov, V. Fuentes-Landete, K. Amann-Winkel, H. Nelson, K. W. Köster, A. I. Kolesnikov, V. N. Novikov, R. Richert, R. Böhmer, T. Loerting, and A. P. Sokolov, Anomalously large isotope effect in the glass transition of water, Proc. Natl. Acad. Sci. USA **111**, 17402 (2014).

[7] C. Beduz, M. Carravetta, J. Y.-C. Chen, M. Concistré, M. Denning, M. Frunzi, A. J. Horsewill, O. G. Johannessen, R. Lawler, X. Lei, M. H. Levitt, Y. Li, S. Mamone, Y. Murata, U. Nagel, T. Nishida, J. Ollivier, S. Rols, T. Rõõm, R. Sarkar, N. J. Turro, and Y. Yang, Quantum rotation of ortho and para-water encapsulated in a fullerene cage, Proc. Natl. Acad. Sci. USA **109**, 12894 (2012).

[8] B. Pamuk, J. M. Soler, R. Ramírez, C. P. Herrero, P. W. Stephens, P. B. Allen, and M.-V. Fernández-Serra, Anomalous Nuclear Quantum Effects in Ice, Phys. Rev. Lett. **108**, 193003 (2012).

[9] L. Lin, J. A. Morrone, and R. Car, Correlated tunneling in hydrogen bonds, J. Stat. Phys. **145**, 365 (2011).

[10] G. Reiter, C. Burnham, D. Homouz, P. M. Platzman, J. Mayers, T. Abdul-Redah, A. P. Moravsky, J. C. Li, C. K. Loong, and A. I.

Kolesnikov, Anomalous Behavior of Proton Zero Point Motion in Water Confined in Carbon Nanotubes, Phys. Rev. Lett. **97**, 247801 (2006).

[11] L. D. Landau and E. M. Lifshitz, *Quantum Mechanics: Non-Relativistic Theory*, A Course of Theoretical Physics Vol. 3 (Pergamon, Oxford, 1965).

[12] M. Benoit, D. Marx, and M. Parrinello, Tunnelling and zero-point motion in high-pressure ice, Nature (London) **392**, 258 (1998).

[13] J. A. Morrone, L. Lin, and R. Car, Tunneling and delocalization effects in hydrogen bonded systems: A study in position and momentum space, J. Chem. Phys. **130**, 204511 (2009).

[14] L. E. Bove, S. Klotz, A. Paciaroni, and F. Sacchetti, Anomalous Proton Dynamics in Ice at Low Temperatures, Phys. Rev. Lett. **103**, 165901 (2009).

[15] J. D. Bernal and R. H. Fowler, A theory of water and ionic solution, with particular reference to hydrogen and hydroxyl ions, J. Chem. Phys. **1**, 515 (1933).

[16] C. Drechsel-Grau and D. Marx, Quantum Simulation of Collective Proton Tunneling in Hexagonal Ice Crystals, Phys. Rev. Lett. **112**, 148302 (2014).

[17] C. Drechsel-Grau and D. Marx, Exceptional isotopic-substitution effect: Breakdown of collective proton tunneling in hexagonal ice due to partial deuteration, Angew. Chem., Int. Ed. Engl. **53**, 10937 (2014).

[18] C. Drechsel-Grau and D. Marx, Collective proton transfer in ordinary ice: Local environments, temperature dependence and deuteration effects, Phys. Chem. Chem. Phys. **19**, 2623 (2017).

[19] O. Benton, O. Sikora, and N. Shannon, Classical and quantum theories of proton disorder in hexagonal water ice, Phys. Rev. B **93**, 125143 (2016).

[20] K. Ueda and M. Oguni, Quantum tunneling in the quadruple proton rearrangement on a hydroxyl hydrogen bond ring in Calix[4]arene, J. Phys. Chem. B **116**, 14470 (2012).

[21] G. Ehlers, A. Podlesnyak, J. L. Niedziela, E. B. Iverson, and P. E. Sokol, The new cold neutron chopper spectrometer at the Spallation Neutron Source: Design and performance, Rev. Sci. Instrum. **82**, 085108 (2011).

[22] G. Ehlers, A. Podlesnyak, and A. I. Kolesnikov, The cold neutron chopper spectrometer at the Spallation Neutron Source - A review of the first 8 years of operation, Rev. Sci. Instrum. **87**, 093902 (2016).

[23] E. Mamontov and K. W. Herwig, A time-of-flight backscattering spectrometer at the Spallation Neutron Source, BASIS, Rev. Sci. Instrum. **82**, 085109 (2011).

[24] O. Arnold, J. C. Bilheux, J. M. Borreguero, A. Buts, S. I. Campbell, L. Chapon, M. Doucet, N. Draper, R. Ferraz Leal, M. A. Gigg, V. E. Lynch, A. Markvardsen, D. J. Mikkelson, R. L. Mikkelson, R. Miller, K. Palmen, P. Parker, G. Passos, T. G. Perring, P. F. Peterson *et al.*, Mantid–Data analysis and visualization package for neutron scattering and μ SR experiments, Nucl. Instrum. Methods Phys. Res. A **764**, 156 (2014).

[25] R. T. Azuah, L. R. Kneller, Y. Qiu, P. L. W. Tregenna-Piggott, C. M. Brown, J. R. D. Copley, and R. M. Dimeo, DAVE: A comprehensive software suite for the reduction, visualization, and analysis of low energy neutron spectroscopic data, J. Res. Natl. Inst. Stand. Technol. **114**, 341 (2009).

[26] S. J. Smith, B. E. Lang, S. Liu, J. Boerio-Goates, and B. F. Woodfieldt, Heat capacities and thermodynamic functions of hexagonal ice from $T = 0.5$ K to $T = 38$ K, J. Chem. Thermodyn. **39**, 712 (2007).

[27] http://energy.gov/downloads/doepublic-access-plan.